



# Alterations of Cowl Lip for the Improvement of Supersonic-Intake Performance

B. John<sup>†</sup> and P. Senthilkumar

*School of Mechanical Engineering, VIT University Vellore, Tamilnadu, 632014, India*

<sup>†</sup>*Corresponding Author Email: [bibin.john@vit.ac.in](mailto:bibin.john@vit.ac.in)*

(Received July 4, 2017; accepted August 9, 2017)

## ABSTRACT

This paper discusses the performance enhancement of supersonic air intake model through the implementation of blunted leading edge to the cowl lip section of the model. A supersonic air intake model with sharp cowl leading edge is initially considered to numerically investigate its performance. Mach 3, supersonic intake flow through the base model has been simulated using commercial CFD package Ansys Fluent-15. Comparison of numerical predictions and experimental measurements is presented to demonstrate the correctness and accuracy of numerical frame work followed in the present study. Higher order spatial accuracy of the solver along with suitably refined mesh helped in accurate capturing of the flow field. Modification to the cowl lip is proposed as an effective method to improve the performance of the supersonic air intake. Two different blunted cowl leading edge geometries were investigated to identify the possible enhancement in performance parameters. Improvement in mass capture and combustion stability attained through the use of forward shifted blunt cowl leading edge is presented. It is also revealed through the present study that the blunt cowl leading edge can reduce the intensity of shock wave boundary layer interaction occurring at the isolator entry section. Deviation in total pressure recovery and flow distortion observed with different supersonic air intake models are also discussed with reasons for the same. This study demonstrates the scope of overall improvement in scramjet engine performance through the use of suitably positioned blunt cowl leading edge.

**Keywords:** Supersonic intake, SWBLI, Flow separation, Mass capture, Total pressure recovery.

## NOMENCLATURE

$CFL$	Courant Friedrichs Lewy number	$p$	static pressure
$h$	isolator throat height	$p_0$	total pressure
$k$	turbulent kinetic energy		
$LE$	leading edge	$\varepsilon$	turbulent dissipation
$M_\infty$	freestream Mach number	$\omega$	specific dissipation
$m$	mass flow rate		

## 1. INTRODUCTION

Shock wave boundary layer interaction is highly undesirable in high speed flow; particularly in high speed air intake systems like ramjet and hypersonic intakes. The successes of such types of air breathing engines are depending upon the intake system and the ability to capture incoming mass with minimum stagnation pressure loss and possible increase in static pressure. Shock wave boundary Layer Interactions (SWBLI) occur due to the close coupling between shock wave and boundary layer in super-sonic flows. They normally arise when a generated shock wave impinges on the surface on which there is boundary layer. These interactions in

a supersonic flow field produce additional shock waves that have its origin within a boundary layer. SWBLI is a region of high pressure and therefore creates an adverse pressure gradient for the boundary layer, leading to its thickening followed by separation. The separation bubble formed due to shock wave boundary layer interaction can decrease the mass capture, total pressure recovery and air intake efficiency. It may also leads to large scale fluctuations like intake buzz and fluctuating side loads. In-creased drag and elevated local heating are other consequences of SWBLI. All these undesired effects can lead to a situation of unstarting of the intake. The turbulence produced is further amplifies the viscous dissipation which leads to in-creased

drag force and decrease in efficiency of an engine. Shock induced separation in a super-sonic inlet creates large areas of separated flow with vortices and increases its unsteadiness and acoustic loads. SWBLIs also increase the aerodynamic contraction which if exceeds the Kantrowitz's limit, will lead to inlet unstart. All of these factors impair the inlets performance and compromise its mechanical integrity.

Size of separation zone is quantitative measure of intensity of shock wave boundary layer interaction. However separation is not always expected in SWBLIs. There should be a minimum SWBLI resulted adverse pressure to ensure separation of the boundary layer, which is known as incipient separation pressure. For turbulent boundary layers, the incipient separation pressure is almost five times of that in case of laminar boundary layers. Moreover, the incipient separation shock angle is directly proportional to the Mach number and is inversely proportional to the Reynolds number (only at lower values). For high Reynolds number, the incipient shock angle is insensitive to changes in Reynolds number.

Shock wave boundary layer interactions involved in the scramjet intake and associated chances of intake under-performance have extensively been studied more than a half century by researchers. The performance improvement by decreasing the intensity of SWBLI in high speed air intake systems is a subject of active research. Many research studies have been reported in literature over many years. Experiments on a planar two-dimensional in-let and isolator geometry operating at Mach 4 with different cowl lengths and angles have been carried out by Emami *et al.* (1995). With the help of interchangeable, rotating cowls of different lengths and isolator sections of different lengths, a total of 250 geometric configurations were tested in this study. Start and unstart predictions were done with the help of static pressure measurements along the ramp and cowl surface. It has been observed from the experiments that the inlet unstarts at approximately the same convergence angle irrespective of cowl lengths. Additionally unstart due to back pressure created by the combustor has been noticed to be depending upon inlet geometry, contraction ratio and isolator length. Later Janarthanam and Babu (2012) have performed computational study employing Emami's intake geometry and experimental conditions. Three different cowl lengths and five cowl convergence angles were re-investigated computationally. It has been identified that the intake unstart is an end effect of SWBLI occurring inside the intake section. The location of shock impingement on the ramp shoulder has seen to be playing an important role in the distortion of the flow at en-try to the isolator. In the same line of thought, Das (Das and Prasad (2010b), Das and Prasad (2010a)) adopted the intake model originally proposed by Necde and Lamb (1965) and carried out both experimental and numerical studies to explore the effects of cowl angle, bleeding of air and angle of incidence on the internal shock characteristics of the in-take and their consequences on starting and

unstarting of the mixed compression intake. Cowl deflection angle has been identified as the parameter that governs the size of separation near the throat region, where the strong shock wave boundary layer inter-action takes place. Experimental study of Koschel and Schneider (1999) is noted as another important research in the field of Scramjet intake design. In this work authors have tested nine different Scram-jet intake models derived from the combination of three different ramp geometries and three different cowl geometries. Similar to other studies of this field boundary layer separation has been found to be affecting the intake performance. Experimental investigations proved that without applying boundary bleed, the ramp side separation bubble generated by cowl lip shock interaction can be minimized by appropriate geometry selection. In a recent experimental work, Mahapatra and Jagadeesh (2008) presented the effects of different contraction ratios in a two dimensional planner intake while operating under a design Mach number of 8. In case of higher contraction ratio, regular shock reflection has been observed with a strong region of separation near to the shoulder region and flow is noticed to be choked. However for lower contraction ratios a shrunk separation region has been obtained. There are many more research papers (Murugan *et al.* 2015; Erdem *et al.* 2013) that dealing with intake design available in the open literature. In all such studies boundary layer separation resulting from the interaction of cowl lip shock with the boundary layer over the ramp surface/isolator wall has been observed to be a key phenomenon that seize the performance of the intake section.

Studies focusing on the suppression of SWBLI induced separation bubble were also reported in the past. Blunting the cowl leading edge has been put forth as an effective means of separation reduction by Lu *et al.* (2014). In this numerical study, four different cowl-lip blunting methods were investigated to understand the flow characteristics of hypersonic intake under the design conditions corresponding 26 km altitude and Mach number of 6. This study showed that Equal Length blunting Manner (ELM) is the most optimal which ensures the minimal total pressure loss, the lowest cowl drag, maximum mass-capture and the minimal aero-heating. The concept of blunt leading edge based SWBLI control has also been demonstrated by Borovoi *et al.* (2011) through their experimental studies. In this work two dimensional interaction between an incident shock and a turbulent boundary layer in the presence of an entropy layer was experimentally investigated by varying plate bluntness and the incident shock position. It has been inferred from this study that the heat transfer to the fluid in the shock incidence zone decreases with increase in the plate bluntness radius. In a subsequent experimental study on air-inlet mounted on a plate kept at Mach number 5 stream (Borovoy *et al.* 2014) reported that even a small bluntness of the plate or the cowl lead to a considerable enhancement of the heat transfer and alterations of SWBLI zone within the airinlet. Later Soltani *et al.* (2015) numerically investigated the unstart suppression in a supersonic intake to study the intake starting problem and

effects of throat area, cowl lip roundness and spike surface curvature upstream of the throat and reported that combinations of these parameters minimize unstart problems and increase intake efficiency also. In a latest study John and Kulkarni (2014) have proved that provision of leading edge bluntness can reduce the flow separation resulting from the SWBLI. A leading edge bluntness radius value higher than the equivalent radius need to be incorporated to ensure separation bubble reduction. Any value of leading edge bluntness lower than the equivalent radius seen to have adverse effect of increasing the separation zone. Final conclusion from the study was that the radius of bluntness should ensure development of boundary layer within strong entropy layer envelop to reduce the intensity of SWBLI. In an associated work, John *et al.* (2016) have also demonstrated that the magnitude of equivalent radius of bluntness is very high for axisymmetric SWBLIs in comparison with that of SWBLIs happening in two dimensional flows.

Research in the field of air intake design has been observed to be very vibrant. Most of the past studies in this field were focusing on the improvement of mass capture and start characteristics of air intakes by considering different combinations of ramps and cowl sections. Researchers have also concentrated on optimizing the contraction ratio to maximize the intake performance. Shock wave boundary layer interactions were observed in all such intake configurations, presence of which significantly reduced mass capture and total pressure recovery of the air intakes. Thus control of SWBLI has been observed to be very crucial to avoid un-start situations of air intakes. Past studies proved that implementation of suitable blunt radius can reduce the intensity of SWBLIs. Very few researchers have tried to implement this concept in hypersonic air intakes. In the same line of thought an attempt is made in this research to control SWBLI occurring in a supersonic air intake by introducing cowl leading edge roundness and positioning. Additional objective of this paper includes identification of improvement in performance parameters of the supersonic air intake model when implementing the cowl bluntness.

## 2. MODEL DETAILS AND FREESTREAM CONDITIONS

A schematic representation of the supersonic air intake base model considered for the present study is shown in Fig.1. This mixed compression intake model was originally proposed by Koschel and Schneider (1999) during their experimental studies focused on analysis of scramjet intake performance. Nine different variance of this model have been tested in their studies. Out of those nine variants, model V-CC is considered for the present study. This model contains an expansion corner followed by two upstream compression ramps. The upper cowl section of the model has a lip which is tilted downward to improve the mass capture. The isolator section of the model is designed with slight divergence to facilitate the acceleration of the super-

sonic flow. This isolator section is provided to prevent the direct interaction of compressed air from intake and the flames from the combustor. The exit of the isolator is assumed to be connected to the combustor inlet.

Free stream conditions considered for the present study are the same as that of test section conditions of Koschel and Schneider (1999) experimental study. Therefore the freestream Mach number has been taken as 3.0 together with freestream static pressure of 15 kPa and static temperature of 135 K. Design of Computational domain has been performed by considering the two dimensional nature of the flow. Grid generation for the accurate prediction of complex flow structure in the mixed compression intake has been experienced to be a critical task in this study. It has been reported that a  $y^+$  value of 100 or less is essential for the accurate prediction of high speed flows (Murugan *et al.* 2015). Moreover, past studies on shock-wave boundary layer interaction phenomenon (John & Kulkarni 2014; John & Kulkarni 2014) clearly showed the utmost importance of local grid refinement in accurate capture of SWBLI affected zone. Upon considering the chances of occurrences of multiple shock wave boundary layer interaction zones both on the ramp surface and in the isolator section, boundary layer meshing has been employed near the solid surfaces. Additional span-wise grid clustering has been applied at different junctions. A representative grid with mentioned kind of refinement is shown in Fig.2. Care has been taken during mesh generation to confirm  $y^+$  value less than one in all the meshes employed for the present study.

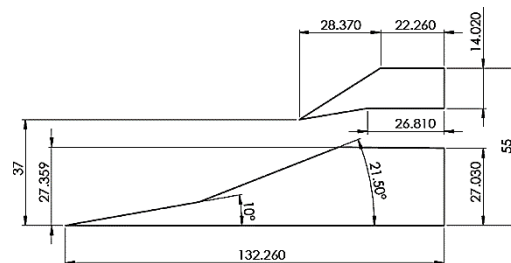


Fig. 1. Dimensions of mixed compression intake geometry (model CC).

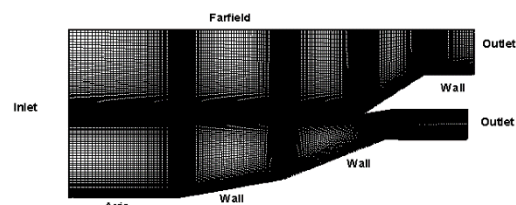


Fig. 2. Sample computational domain marked with boundary conditions.

With the consideration of supersonic flow physics, boundary conditions were applied to different boundaries of the computational domain. The inlet boundary of the domain has been taken as supersonic inlet and freestream conditions were assigned to the inlet cell faces. Turbulent intensity of 5% has been

specified at the inlet of the do-main. For an undisturbed freestream entering to the inlet of an internal flow domain, the turbulent intensity can be fairly high with values ranging from 1%– 10%. Hence 5% inlet turbulent intensity considered for the present simulation is an adequate choice. Farfield boundary has also been set with freestream conditions by selecting pressure farfield boundary condition available in Fluent solver. Out-let has been treated as supersonic outlet (pressure outlet). All the wall boundaries were set with adiabatic no-slip boundary condition. Axis boundary was treated as symmetry plane.

### 3. COMPUTATIONAL METHODOLOGY

Integral form of two dimensional compressible flow governing equations were solved in each cells of the computational domain discussed in the previous section by employing commercial finite volume solver Fluent 15. To ensure the closedness of the continuity, momentum and energy equations, the fluid is assumed to be ideal gas and equation of state is applied. Additionally  $k - \epsilon$  turbulent model with standard wall function has been used to model the turbulent flow. AUSM (advection up-stream splitting method) upwind scheme which offers best trade-off between dissipation and accuracy for high speed flow simulations (John *et al.* 2014) has been employed for inviscid flux calculations. Green-Gauss cell based gradients are used for the computation of viscous flux terms. Prediction of complex supersonic flow features requires higher order spatial accuracy. Hence second order reconstruction has been used for the computation of wall properties. A CFL number of 0.5 or less has been chosen for the reason of stability. All the simulations were targeted for steady state results. Hence proper selection of convergence criterion has been noticed to be vital for the confirmation of steady state. During the present simulations, scaled residuals of mass, momentum, energy and turbulent parameters have been considered to analyze the convergence of the solution. Solution has been assumed to be steady when the residual of density has fallen below  $10^{-6}$ . For compressible flow simulations, it is a general observation that convergence of continuity will ensure convergence of all other residuals. Although convergence of all residuals below  $10^{-6}$  has been expected, complexities involved in the flowfield made the residuals to stall between  $10^{-4}$  and  $10^{-6}$  in some of the present simulations. However in the cases where stalling of residuals observed, time marching has been continued for prolonged time to ensure that there are no further alterations in the field and surface parameters. Hence the results discussed in the subsequent sections are all steady state values.

### 4. RESULTS AND DISCUSSIONS

#### 4.1 Validation and Grid Independence Study

Validation of the numerical frame work adapted for the study is essential to rely on the results obtained

from the numerical simulation. Addition-ally grid independence study has to be performed to ensure the absence of grid based error in the numerical solution. Hence, initially a validation come grid independence study has been performed for the supersonic air intake model by employing freestream conditions mentioned in the previous section. Three different levels of meshing have been considered during this study. The computational domain has been initially meshed with 14450 quadrilateral cells. For this coarse grid the first cell height near the wall was set to  $4 \times 10^{-6}$  m. The next level of grid (medium grid) contained 58500 quadrilaterals with a first cell height of  $2 \times 10^{-6}$  m. Finally the third level mesh (fine grid) has been generated with 128580 cells by setting first cell height near the wall equal to  $1 \times 10^{-6}$  m. For all three grid levels adequate grid clustering has also been provided near ramp junctions and leading edge regions. The variation of  $y^+$  along the non-dimensional flow axis ( $x/h$ ) on different wall surfaces of the medium grid is shown in Fig. 3. It is evident from this figure that the  $y^+$  values are less than one at the isolator walls, where SWBLs are expected. Slightly higher values of  $y^+$  near the leading edges of ramp and cowl sections are due to sudden growth of boundary initiated at those regions. Moreover, the well behaved nature of boundary layer on those surfaces does not re-quire very low  $y^+$  values over there. Oscillations observed in the  $y^+$  distributions on isolator top and bottom walls can be attributed to shock wave boundary layer interactions occurring at those sections.

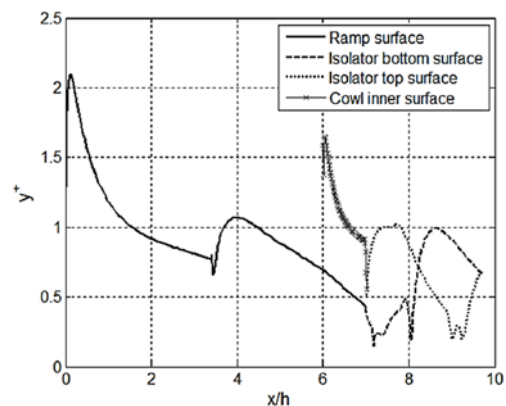


**Fig. 3. Variation of  $y^+$  values on the walls of ramp, cowl and isolator sections of base model.**

Results obtained on such suitably meshed do-main are further subjected to validation. For the validation purpose the ramp-surface pressure distributions obtained from different levels of grid are compared with experimental measurements and re-ported numerical predictions in Fig. 4. It is very clear from this figure that the present numerical results are in good agreement with experimental data. Moreover the surface pressure distributions obtained on medium and fine grids are very close, which supports the grid independent nature of the solution. Further to ascertain the grid independence of the solution in terms of viscous parameters, the variation of stream wise velocity normal to the isolator bottom wall at  $x$

= 0.013m is compared in Fig. 5. This location ( $x = 0.013m$ ) is chosen for the comparison because of the fact that the core of separation zone resulting from SWBLI over the isolator bottom wall lies at this location. It is again evident from Fig. 5 that the velocity profile predictions on two higher level grids are very close as compared to that of coarse grid. Further the comparison of present results with literature reported numerical data also reasonably matches. Slight disparity in pressure values in the isolator section can be attributed to the difference in turbulent models and quality of mesh used for the studies.

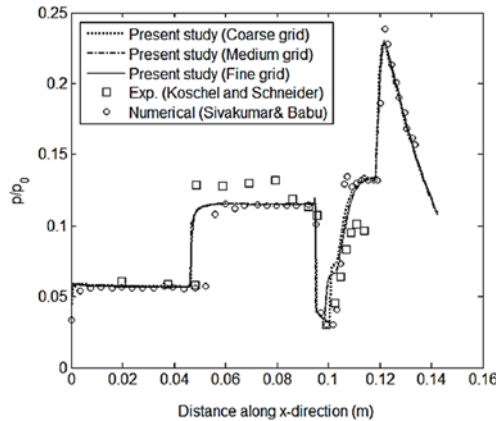


**Fig. 4. Comparison of surface pressure distribution over the ramp surface.**

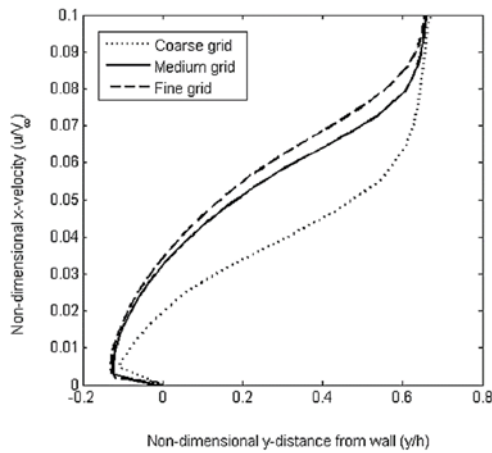


**Fig. 5. Comparison of velocity distribution in the separation zone at  $x=0.0103$  m away from the leading edge of the model.**

Importance of selection of adequate turbulent models for high speed flow simulations has been re-reported in the works of Huang *et al.* (2013). Therefore to defend the use of  $k - \epsilon$  turbulent model along with standard wall function for the current study, it has been decided to repeat the simulation on medium level grid with SST  $k - \omega$  turbulent model. Further to investigate the effect of different turbulent models on the numerical solution, comparison of surface pressure distributions has been considered. Thus the surface pressure distributions predicted by two turbulent models are compared in Fig. 6. Additionally, the current numerical predictions are also compared with literature reported numerical and

experimental data. This comparison made on the ramp surface shows that the prediction of  $k - \epsilon$  turbulent model with standard wall function is superior over the solution obtained with the second turbulent model considered in the present study. Moreover, it is very clear from Fig. 6 that the separation zone predicted by  $k - \omega$  model is not matching with experimental measurements. Further comparison of pressure variation on the upper cowl surface (Fig. 7) also reveals the inaccuracy of  $k - \omega$  model for the accurate modeling of near wall flows under considered grid and flow conditions. The close match of experimental measurements and numerical predictions obtained while using “ $k - \epsilon$  turbulent model coupled with standard wall function,” has encouraged to proceed the further simulations with the same turbulent model. However, to comment on the most accurate turbulent model for the similar flow situation; further investigation is to be carried out. Finally, the close matching nature of experimental and numerical results supports the validity and accuracy of present numerical frame work.

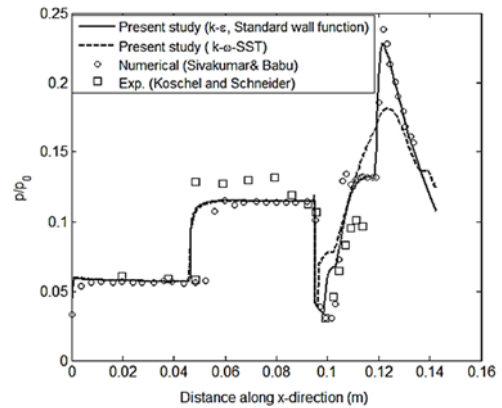


**Fig. 6. Comparison of surface pressure distribution predicted by different turbulent models.**

In addition to the pressure distributions, numerical schlieren images of supersonic flow through the air intake are considered further to clearly demonstrate the various flow features. The schlieren image of the flow through the base model is shown in Fig. 8. This figure visualizes two compression waves emanating from the first and second ramp foots. These two oblique shock waves are interacting with the cowl leading edge shock at a location little away from the leading edge of the cowl section. If these upstream compression waves hit the cowl section exactly, then maximum mass capture is possible and at that case the intake is said to be in critical mode of operation. However the present simulation as well as past experimental study have demonstrated that the considered condition is a subcritical operation mode. So the mass capture is slightly lower than the maximum possible value. The captured mass flow is seen to be passing across right running cowl-shock before entering the isolator, hence attaining further pressure rise. However, close to the bottom isolator wall, the cowl shock interacts with the centered expansion fan, thus weaken in strength. It is very evident from Fig. 8 that the fluid particles within the

bottom half of the isolator section have first experienced expansion wave and then encountered the weakened compression wave; whereas the fluid particles confined to the upper half of the isolator have crossed the compression wave first and then expansion wave. This fact can also be noticed from the disparity in the pressure distributions on the ramp and cowl surfaces. The interaction of weakened cowl shock with the boundary layer developing over the bottom isolator wall has resulted in local separation of the flow. This flow separation zone is also marked in the schlieren map. It is apparent from the Fig. 8 that the separated flow further reattaches by passing across a reattachment shock. Subsequent interaction of this reattachment shock with boundary layer developing on the upper wall of the isolator is also visible in the schlieren image. Additional shock generated by the cowl-deflector end and its interactions are also shown in Fig.8. The asymmetric shock structure and their interactions with boundary layer on the upper and lower isolator walls result in non-uniform flow at the isolator exit. The isolator section is seen to be rising the static pressure of the flow to the required combustion pressure limit by allowing the flow to pass across multiple shock trains. However, the specific design of the isolator does not allow the flow to decelerate down to subsonic regime. Hence, in the absence of frictional choking the flow at the exit of the isolator is maintained to be high pressure supersonic flow.

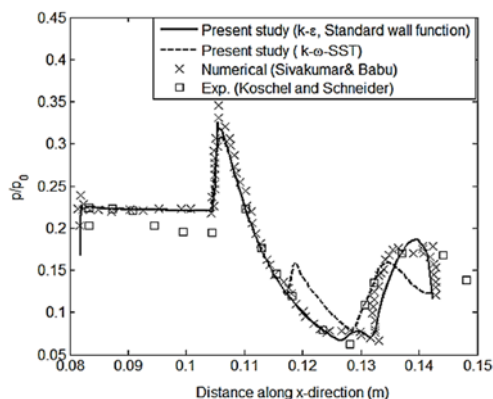


**Fig. 7. Comparison of surface pressure distribution over the cowl and isolator upper wall surface.**

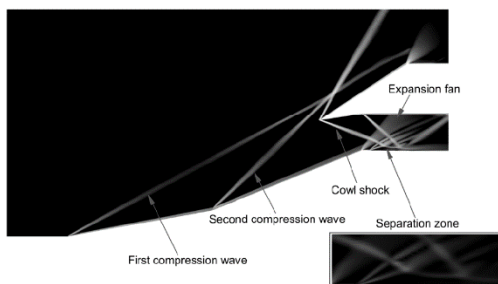


**Fig. 8. Schlieren map showing various flow features of the base model.**

**4.2 Performance improvement using blunted cowl leading edge.**

The performance of the supersonic air intake will

improve if the mass capture can be increased by some means. Additionally the isolator exit Mach number and pressure are to be maintained as high as possible. The present study focuses on achieving these enhancements through the re-placement of sharp cowl-leading edge with a blunt cowl-leading edge. Hence a blunt leading edge of radius 0.5 mm is introduced to the cowl lip. Two different blunt leading edge cases were considered for this study. In the first case 0.5 mm bluntness has been achieved just by making fillet to both up-per and lower surface of the cowl. This ended up in a slightly backward shifted cowl lip in comparison with sharp leading edge section of original model. Here after this case of geometry is referred as ‘blunt cowl LE-default location’. In the second case of blunt leading edge model, the blunted cowl section has been pushed forward to match with actual leading edge location of base model. This second modified scramjet intake model is mentioned as ‘For-ward shifted blunt cowl LE’ for the rest part of this paper. The blunt cowl leading edge is observed to be resulting in the formation of a detached shock in front of the cowl. This is apparent from the schlieren images presented in Fig. 9 and 10. Irrespective of location of the blunt leading edge, the shape of the bow shock is observed to be nearly the same for both the cases. This observation has to be attributed to the fact that, the blunt leading edge is exposed to almost same flowfield (flowfield containing fluid particles that have crossed both the up-stream compression waves) in either case. Due to the change in orientation of the bow shock resulted from the detached nature, the shock boundary layer interaction location is noticed to be shifting for-ward on the lower isolator surface. Moreover, the SWBLI resulted separation zone size is seen to be very negligible. This is very clear from the surface pressure comparison presented in Fig. 11. In this pressure distribution all three geometry cases have same trend till the post expansion fan location. Behind the centered expansion fan the pressure distributions depart each other. A near plateau region in the pressure plot just after the expansion fan region can be taken as a parameter to quantify the intensity of separation. Hence it can be concluded from Fig. 11 that the highest separation bubble exist in case of sharp leading edge model.

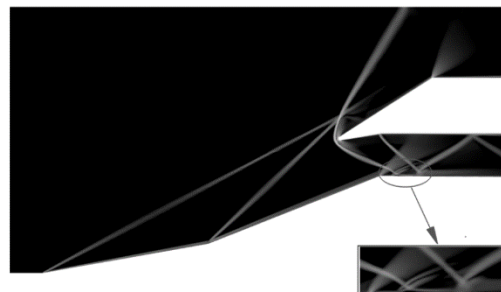


**Fig. 9. Schlieren image obtained with blunt cowl leading edge-default location model.**

Separation zone size is minimum in case of Forward shifted blunt cowl LE. Separation bubble size of blunt cowl LE- default location lies in between the sizes obtained with other two cases.

Reduced nature of separation is advantageous in aerodynamic point of view, as it reduces the total pressure drop. So, local aerodynamic gain is assured through the use of blunted leading edge. Although the shock emanating from the aft section of cowl-deflector also hits the isolator lower wall, it does not lead to local flow separation. However this shock is noticed to be reflecting back by leaving a small Mach stem near the isolator wall. The last abrupt jump in pressure distribution is caused due to the presence of this Mach stem. The pressure peak attained across this Mach stem is seen to be highest in case of forward shifted blunt cowl leading edge case. Beyond this pressure peak, surface pressure is de-creasing due to boundary layer thickening as in case of flow over a flat plate. This decreasing trend is al-most similar in all three cases.

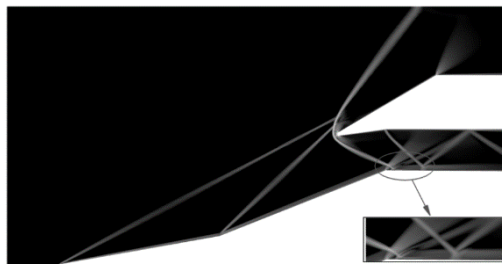


**Fig. 10. Schlieren image obtained with forward shifted blunt cowl leading edge model.**

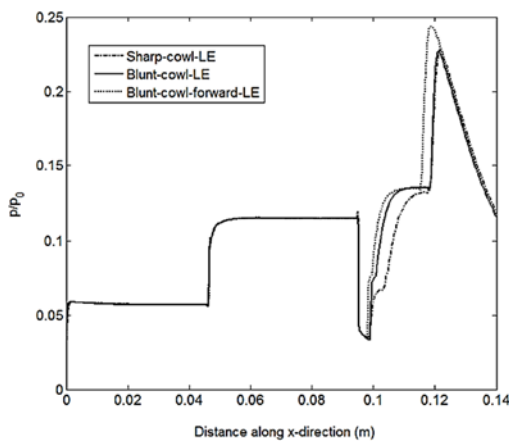


**Fig. 11. Comparison of surface pressure distribution over the ramp surface obtained with different cowl leading edge modifications.**

To explain the physics behind the blunt leading edge based separation reduction, density con-tours of flow through three different geometries of present interest are compared in Fig. 12. Stream-lines are overlapped on the density contours to visualize the flow pattern under different leading edge conditions. Comparison of different density maps shows that the peak density in the blunt domains is almost 1.5 times higher as that of sharp domain. The high density regions exit in front of the stagnation point of blunted cowls. The absence of bow shocks limit the peak density value of sharp cowl domains well below that of domains

with blunt cowl leading edge. Moreover, the presence of bow shock creates a non-uniform variable density flow behind it. Hence the directions of streamlines are not the same behind the curved shock as op-posed to streamlines of identical slope observed in case of oblique shock. This disparity of flow structure and streamlines are very clear in Fig. 12. The density contours of blunt leading edge cases show that the location of impingement of cowl shock on the isolator bottom wall shifts forward with cowl leading edge alteration. The shift of SWBLI location observed with “ blunt cowl LE- default location” is due to the change of orientation of the cowl shock. Whereas, the change in SWBLI location in case of Forward shifted blunt cowl LE is due to cowl shock recasting as well as cowl leading edge repositioning. As the shock impingement location moves forward on the isolator surface, the thickness of boundary layer to which the shock interacts can be seen to be reducing. Thinner boundary layer will have higher stability against adverse pressure gradient. This could be one of the possible reasons of reduced flow separation observed with blunt cowl leading edge geometries. Another interesting observation from the Fig. 12 (a) is that the streamlines have higher slope in the downstream region of oblique cowl shock and are deviating away from the separation zone. However, in case of “For-ward shifted blunt cowl LE” geometry majority of the streamlines are either parallel to the isolator bot-tom wall or with lesser upward deflection as com-pared to post cowl shock streamlines of sharp leading edge geometry. Hence, in the case of blunt cowl models, the main stream flow will force the decelerated boundary layer flow to be attached to the surface of the isolator. In addition to above discussed facts, the inviscid vorticity resulting from the density gradient of curved shock layer may also offer resistance to shock induced flow separation.

### 4.3 Analysis of Bluntness Induced Parametric Alterations at the Isolator exit

Any improvement in intake performance must be reflected at the isolator exit conditions. So the performance parameters are analyzed at the isolator exit section to portray the improvements brought in by the modified cowl leading edge cases. Variation of total pressure across the isolator exit plane is compared in Fig. 13. The total pressure values are almost same for the bottom half of the cowl exit. Towards the mid-section of the isolator exit, total pressure values obtained with blunted cowl leading edge cases are overshooting the same of sharp leading edge geometry. However considerable drop in total pressure can be observed near the upper wall of isolator for blunt leading edge models. It should be noted that the upper half of the isolator receives fluid that has crossed the strong region of cowl leading edge bow shock. That is the reason for total pressure departure near the isolator upper surface, in case of blunted geometries in Fig. 13.

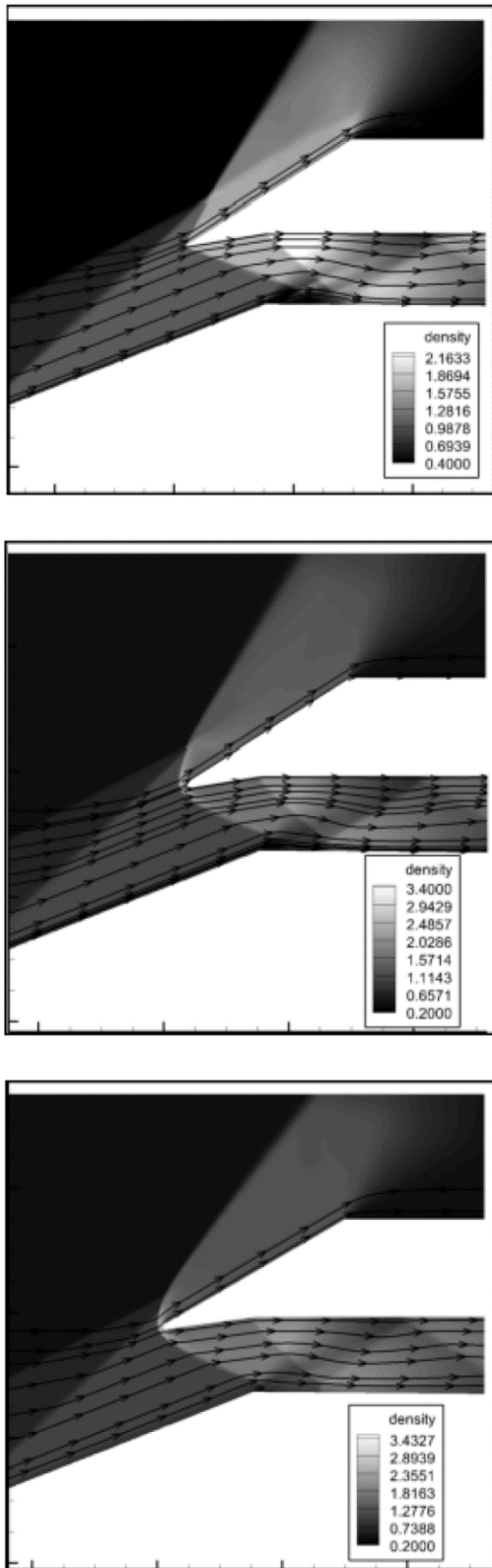


**Fig. 12.** Density contours overlapped with stream-lines for (a) Sharp cowl geometry, (b) blunt cowl LE- default location and (c) Forward shifted blunt cowl LE.

Although blunted cowl lips are not considerably improving the performance in terms of exit total pressure, the static pressure enhancement at the isolator exit is very significant in those cases. This is

evident from Fig. 14. For the entire isolator exit section, the static pressure values are substantially higher in case of forward shifted blunt cowl leading edge case in comparison with the values recorded for other two models. For major portion of the isolator exit, static pressure values obtained with sharp cowl model lies below that of blunt leading edge models. Since higher pressure at the combustion chamber helps in efficient combustion, it can be concluded based on Fig. 14 that the forward shifted blunt cowl leading edge geometry out performs other two in terms of isolator exit static pressure (which is expected to be the combustion pressure).

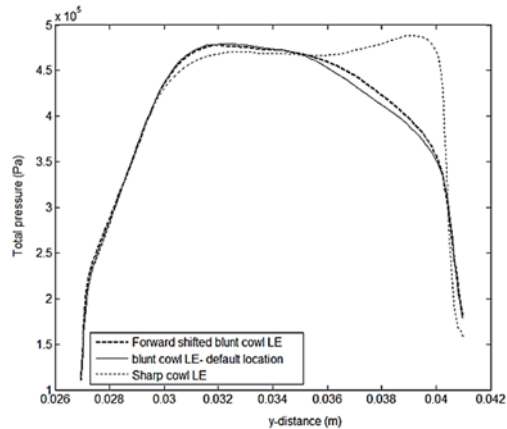


**Fig. 13.** Comparison of total pressure variation across the isolator exit obtained with different cowl leading edge modifications.

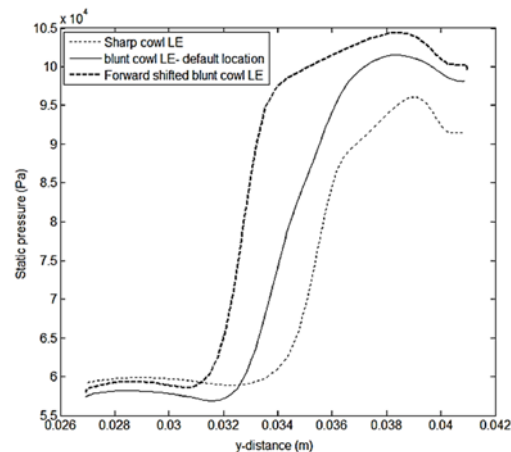


**Fig. 14.** Comparison of static pressure variation across the isolator exit obtained with different cowl leading edge modifications.

Supersonic combustion needs supersonic flow in the combustion chamber. The Mach number distributions obtained at the isolator exits of different scramjet intake models are compared in Fig. 15. It can be seen from this figure that the Mach numbers at the isolator exit are slightly lower for blunted leading edge models in comparison with the same obtained for sharp leading edge intake model. Although the average isolator exit Mach number value is noticed to be little low for blunt leading edge models, the maximum value of isolator exit Mach number still belongs to blunt leading edge model.

**Table 1 Comparison of total pressure recovery and flow distortion**

	Total pressure recovery	% drop in total pressure	Flow distortion
Sharp cowl LE	0.655	—	1.0436
Blunt cowl-default location	0.643	1.83	1.0365
Forward shifted blunt cowl LE	0.629	3.97	1.0592

Moreover moderate combustion chamber Mach number is best suited for effective and stabilized combustion. In that point of view, slightly dropped value of average isolator exit Mach number is expected to have favorable effect in scramjet engine performance.

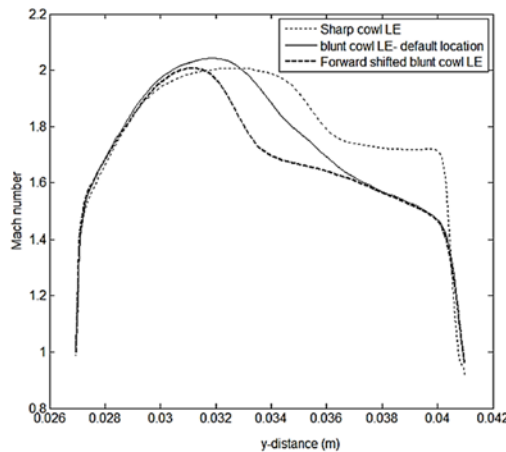


**Fig. 15. Comparison of Mach number variation across the isolator exit obtained with different cowl leading edge modifications.**

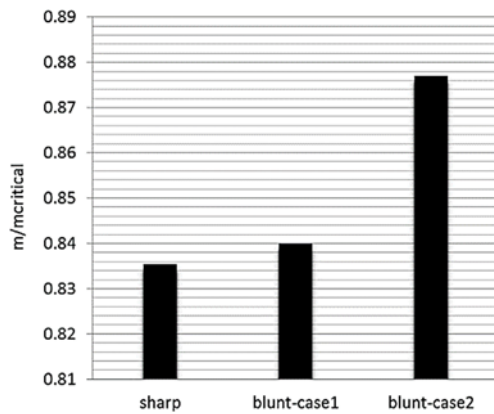


**Fig. 16. Comparison of mass flow rate at the exit of the isolator.**

The mass flow rates calculated at the isolator exit are analyzed in Fig. 16. This figure reveals that the blunted cowl leading edge can improve mass capture. The critical mass flow rate considered for normalizing the mass capture is calculated by assuming the critical mode of operation of sharp cowl leading edge model. The model with default blunt leading edge location has not improved the mass capture considerably. Only less than 1% enhancement is noticed in that case. Whereas forward shifted blunt cowl leading edge model

increased the mass capture by 5%. This is a positive sign of performance enhancement. This increased mass flow rate indeed improves the thrust generated by the engine. Noticed mass flow enhancement has to be correlated to modified flow structure at the cowl lip region. In fact the blunted leading edge, relocated to the actual leading edge location of original model turns more flow in to the isolator section. That is how the improvement in mass capture achieved. So it can be inferred that suitably located blunt cowl leading edge can outperform sharp leading edge model in magnitude of mass capture.

Finally total pressure recovery and flow distortion are computed to compare the relative advantage of various inlet designs. Here the total pressure recovery is calculated as,

$$\text{Total pressure recovery} = p_{0avg} / p_{0\infty}$$

Where  $p_{0avg}$  is the average value of total pressure at the isolator exit and  $p_{0\infty}$  is the freestream total pressure. Thus calculated values of total pressure recovery are tabulated in Table.1

It is evident from Table. 1 that the total pressure recovery is slightly dropped in cases of blunted leading edge models. Almost 1.83% reduction in total pressure recovery is observed with “blunt cowl default location” model, whereas the drop is little higher in case of forward shifted blunt cowl leading edge model. For that model the total pressure recovery is dropped from 0.655 of original model to 0.629. This observation points to the fact that the increase in mass flow rate is possible only with the expense of slight drop in total pressure recovery.

It is also meaningful to look into flow distortion caused with different scramjet intake designs. Flow distortion is a representative that talks about non-uniformity of the flow at the isolator exit. In the present study this parameter is calculated as,

$$\text{Flow distortion} = \frac{P_{0max} - P_{0min}}{P_{0mean}}$$

Efficient intake is expected to offer minimum flow distortion at the isolator exit. It is clear from Table. 1 and Fig. 17 that the flow distortion is minimum in case of blunt cowl leading edge at default location. Flow distortion observed with forward shifted blunt cowl leading edge model is higher than that of other two models. However, authors are of the opinion that the under performance of forward shifted blunt cowl leading edge model in terms of slightly dropped pressure recovery and enhanced flow distortion can be compensated by improvement in mass capture and combustion chamber pressure.

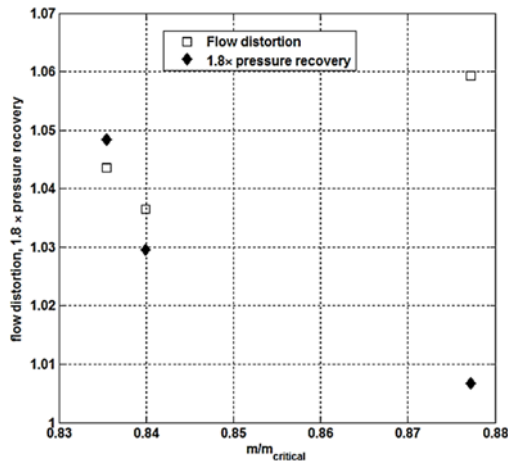


Fig. 17. Comparison of flow distortion and pressure recovery.

## 5. CONCLUSIONS

Numerical investigation of sub-critical operation of multiple-compression supersonic air intake model is presented. Comparison of present numerical predictions with earlier reported experimental measurements and computational results have showed excellent agreement. That demonstrated the accuracy and capability of numerical frame work opted for the present study. Utmost importance of local grid refinement for the accurate prediction of flow features, especially shock wave boundary layer interaction zones is identified through the present study. It has been observed that under sub-critical mode of operation original air intake model with sharp cowl leading edge results in a quite large separation zone in the isolator bottom wall. Clearly visible nature of pressure plateau in the lower wall pressure distribution stands to support this observation. An effort has been taken to investigate the performance enhancement of supersonic air intake model by altering the cowl leading edge condition. Instead of sharp cowl leading edge, blunted leading edge of 0.5 mm radius is considered for this study. Two different variants of supersonic air intake model with blunted cowl have been analyzed. Introduction of leading edge bluntness to the cowl lip of first modified model is achieved by simply filleting the upper and lower cowl surfaces. This resulted in slightly aft shifted cowl leading edge location. In the second variant of the scramjet intake model, the blunted cowl has been shifted forward to match with leading edge location of original model to compensate the slightly shortened nature of cowl. Numerical investigations have been carried out for both the modified intake models using the same numerical frame work. During this study care has been taken to suitably refine the grid as in the case of sharp leading edge model.

Comparison of schlieren maps and surface pressure distributions obtained from the simulations of blunt models with that of sharp cowl leading edge model clearly demonstrated the reduced nature of SWBLI caused separation on the isolator wall. The reduced nature of separation zone is correlated to aft movement of SWBLI location and increased flow

stability offered by inviscid vortices in the curved shock layer. Moreover the performance assessment in terms of calculated values of performance parameters at the isolator exit showed the improvement in combustion pressure and mass flow rate while using the blunted leading edge models. Almost 5% improvement in mass capture has been noticed with forward shifted blunt cowl leading edge model. Comparison of Mach number distributions across the isolator exit section demonstrated that the average isolator exit Mach number marginally drops while implementing the blunted cowl section. However this drop may help in improving the combustion stability, thus results in efficient combustion and enhanced thrust delivery. Marginally dropped total pressure recovery is identified as a drawback of blunted cowl leading edge geometries. Flow distortion comparison showed least flow distortion in case of blunted cowl leading edge at the default location. The forward shifted blunt cowl leading edge model has been marked with maximum flow distortion among the considered cases.

Thus the present study hints about the scope of improving the performance of scramjet intakes through the implementation of blunted cowl leading edge section. The present study predicts an overall improvement in scramjet performance due to enhanced mass capture and combustion stability with the penalty of slightly dropped total pressure recovery in case of forward shifted blunt cowl leading edge model. The other blunted model shows only trivial improvement in the performance. However the flow distortion is noticed to be the minimum for this model. Hence it is expected that the best tradeoff between mass capture enhancement and flow distortion can be achieved by choosing an optimum leading edge location in between the present considered locations. Moreover the performance would be different for a varied leading edge bluntness radius, which is to be investigated further. It can also be inferred from the present study that extension in isolator length may reduce the flow distortion at the inlet to the combustion chamber.

## REFERENCES

- Borovoi, V. Y., I. Egorov, A. Y. Noev, A. Skuratov and I. Struminskaya (2011). Twodimensional interaction between an incident shock and a turbulent boundary layer in the presence of an entropy layer. *Fluid Dynamics* 46(6), 917–934.
- Borovoy, V. Y., V. Mosharov, V. Radchenko, A. Skuratov and I. Struminskaya (2014). Leading edge bluntness effect on the flow in a model air-inlet. *Fluid Dynamics* 49(4), 454–467.
- Das, S. and J. Prasad (2010a). Starting characteristics of a rectangular supersonic air-intake with cowl deflection. *The aeronautical journal* 114(1153), 177–189.
- Das, S. and J. Prasad (2010b). Unstart suppression and performance analysis of supersonic air-intake adopting bleed and cowl bending. *IE (I) Journal-AS* 91, 27–35.

- Emami, S., C. A. Trexler, A. H. Auslender and J. P. Weidner (1995). Experimental investigation of inlet-combustor isolators for a dual-mode scramjet at a mach number of 4, Report number: NASA-TP-3502.
- Erdem, E., K. Kontis, E. Johnstone, N. Murray and J. Steelant (2013). Experiments on transitional shock wave-boundary layer interactions at mach 5. *Experiments in fluids* 54(10), 1598.
- Huang, W., S.-b. Li, L. Yan and Z. g. Wang (2013). Performance evaluation and para-metric analysis on cantilevered ramp injector in supersonic flows. *Acta Astronautica* 84, 141–152.
- Janarthanam, S. and V. Babu (2012). Numerical simulations of the flow through the inlet and isolator of a mach 4 dual mode scramjet. *The Aeronautical Journal* 116(1182), 833–846.
- John, B. and V. Kulkarni (2014). Effect of leading edge bluntness on the interaction of ramp induced shock wave with laminar boundary layer at hypersonic speed. *Computers & Fluids* 96, 177–190.
- John, B., G. Sarath, V. Kulkarni and G. Natarajan (2014). Performance comparison of flux schemes for numerical simulation of high-speed inviscid flows. *Progress in Computational Fluid Dynamics, an International Journal* 14(2), 83–96.
- John, B., S. Surendranath, G. Natarajan and V. Kulkarni (2016). Analysis of dimensionality effect on shock wave boundary layer interaction in laminar hypersonic flows. *International Journal of Heat and Fluid Flow* 62, 375–385.
- Koschel, W. and A. Schneider (1999). *Detailed analysis of a mixed compression hypersonic intake*. In Fourteenth International Symposium on Air Breathing Engines. AIAA.
- Lu, H., L. Yue and X. Chang (2014). Flow characteristics of hypersonic inlets with different cowl-lip blunting methods. *Science China Physics, Mechanics and Astronomy* 57(4), 741–752.
- Mahapatra, D. and G. Jagadeesh (2008). Shock tunnel studies on cowl/ramp shock interactions in a generic scramjet inlet. Proceedings of the Institution of Mechanical Engineers, Part G: *Journal of Aerospace Engineering* 222(8), 1183–1191.
- Murugan, T., S. De and V. Thiagarajan (2015). Validation of three-dimensional simulation of flow through hypersonic air-breathing engine. *Defence Science Journal* 65(4), 272–278.
- Neale M. C. and Lamb P. S. (1965). Tests with a variable ramp intake having combined external/internal compression, and a design Mach number of 2.2, *Aeronautical Research Council – CP*. 805.
- Soltani, M., J. S. Younsi and V. F. Khanaposhtani (2015). Numerical investigation of the unstart suppression in a supersonic air in-take. *Iranian Journal of Science and Technology. Transactions of Mechanical Engineering* 39(M2), 413.